Title: Looking for non-dark matter: Sunyaev-Zeldovich-gravitational-lensing cross correlations

Date: Mar 10, 2015 11:00 AM

URL: http://pirsa.org/15030106

Abstract: Visible matter consists mostly of hydrogen and helium, only a small fraction
of which is in stars. Until recently, the bulk of the gas in the local
universe was in fact not seen. In the largest structures, massive galaxy
clusters, the gas is seen via its x-ray emission, but in the much more
numerous groups and isolated galaxies, it has not been possible to detect
it. I will describe how, in the last year or so, the situation has changed,
with the detection of a cross-correlation between the thermal SZ effect and
lensing maps, and through the stacking of SZ images at the locations of
galaxies. These and similar techniques will tell us about the physics by
which stars and massive black holes heat and move gas in and around the
halos of galaxies and cluster, and will allow for tighter constraints on the
value of the primordial power spectrum (sigma_8).


Looking for non-Dark Matter
Sunyaev-Zeldovich-gravitational-lensing cross correlations
Nick Battaglia, Colin Hill, Ludo van Waerbeke, Gary Hinshaw

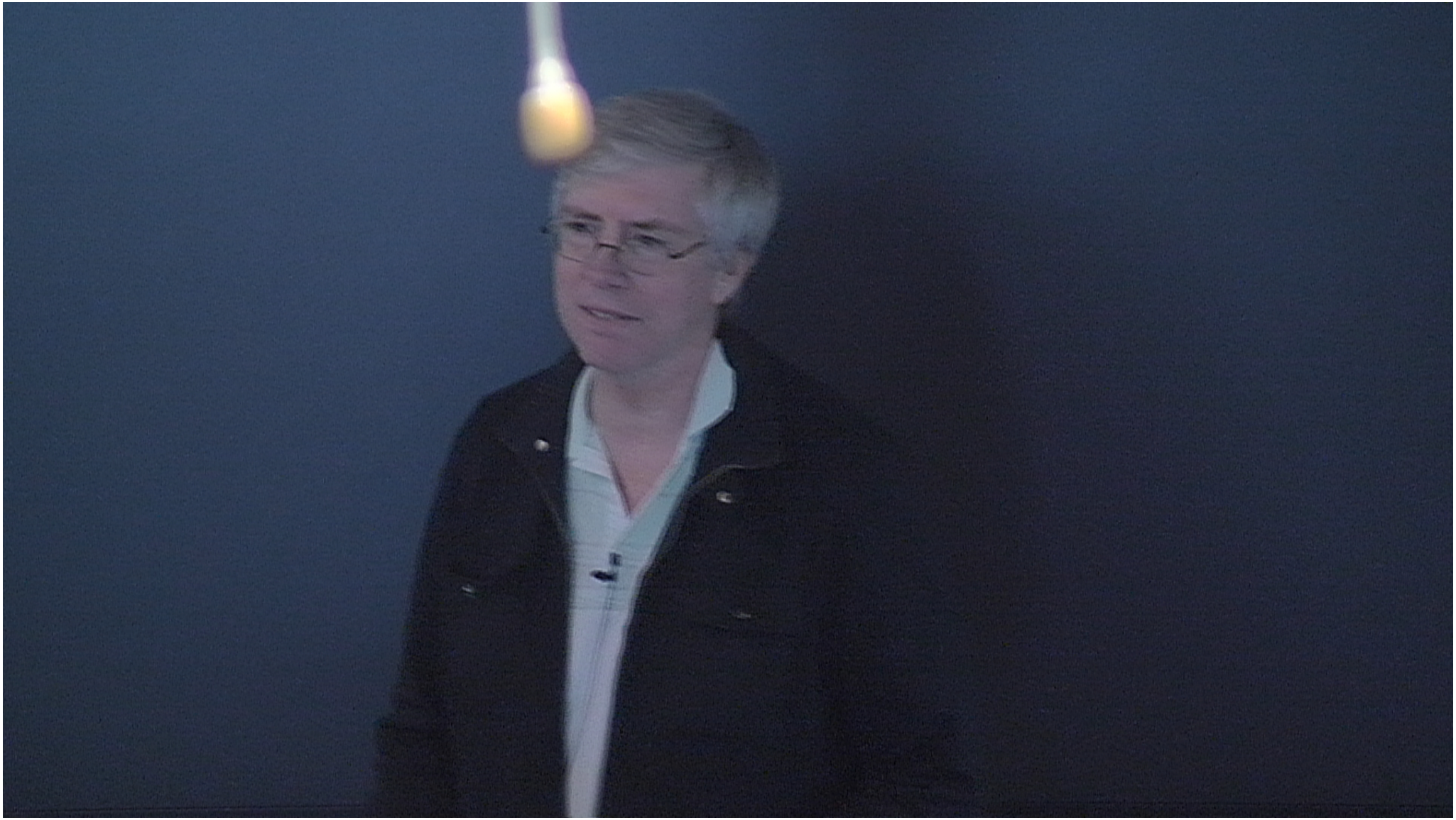

Looking for non-dark matter

- Astronomers and (especially) cosmologists believe in dark matter
  - We can look outside and see luminous matter
  - But the luminous matter we see around galaxies doesn't add up—-there is a "missing baryon"
- Does ΛCDM really work?
- Simulations
- Observations of both dark and baryonic matter
- Constraints on cosmological parameters: σ_8

Cold dark matter, the structure of galactic haloes and the origin of the Hubble sequence

Carlos S. Frenk*, Simon D. M. White†, George Efstathiou‡ & Marc Davis§

* Astronomy Centre, University of Sussex, Brighton BN1 9QH, UK
† Steward Observatory, University of Arizona, Tucson, Arizona 85721, USA
‡ Institute of Astronomy, Madingley Road, Cambridge CB3 0HA, UK
§ Astronomy Department, University of California, Berkeley, California 94720, USA

A popular theory for galaxy formation holds that the Universe is dominated by exotic particles such as axions, photinos or gravitinos (collectively known as cold dark matter, CDM)[1–3]. This hypothesis can reconcile the aesthetically pleasing idea of a flat universe with the standard theory of primordial nucleosynthesis and with upper limits on anisotropies in the cosmic microwave background[4–6]. The resulting model is consistent with the observed dynamics of galaxy clustering only if galaxy formation is biased towards high-density regions[7,8]. We have shown that such a biased model successfully matches the distribution of galaxies on megaparsec (Mpc) scales[9]. If it is to be viable, it must also account for the structure of individual galaxies and their haloes. Here we describe a simulation of a flat CDM universe which can resolve structures of comparable scale to the luminous parts of galaxies. We find that such a universe produces objects with the abundance and characteristic properties inferred for galaxy haloes. Our results imply that merging plays an important part in galaxy formation and suggest a possible explanation for the Hubble sequence.

The morphology of most galaxies can be represented as a superposition of a rotationally supported disk and an ellipsoidal stellar system. The Hubble sequence classifies galaxies according to the relative importance of these components. Spiral bulges and faint ellipticals show substantial rotation, but most bright ellipticals rotate slowly[10]. Further, ellipticals are found preferentially in regions of high galaxy density whereas spirals avoid such regions[11]. Spirals are surrounded by unseen massive haloes which are responsible for the flat rotation curves of their outer disks[12]; little is known about the mass distribution surrounding ellipticals. These systematic properties of galaxies and the associated characteristic scales are the least that any theory of galaxy formation should explain. Below we show that, at this level, a flat CDM universe provides an attractive arena for galaxy formation.

are no further free adjustable p
tion. The model contains 2 ×
32,768 particles. In the real U
average, about 2 galaxies brig
brighter than M33. Our code
correctly on scales larger than
This resolution limit correspon
at the end of the calculation.

The left-hand panels of Fig.
of structure in our model. By a
with circular speeds exceeding
high peaks of the initial linear
circular speeds >200 km s^{-1}.
centrally concentrated. Betwe
of them remain isolated and
while others merge into larger
evolution of three large clu
sequence of mergers, anothe
merging at the end of the sim
relative isolation. The inner
smooth and significantly tria
effectively erased the structure
of the large asymmetries prese
of the angular momentum inve
subclumps to outlying materia
example, the most bound 20%
loses 70% of its angular mom
between a redshift of 1 and th

Figure 2 shows the circula
radius (r) for the 10 largest
present day. These curves are
resemble the measured rotati
spiral galaxies. Observed rotati
ably smaller radii than we ca
calculation. However, unpub
Barnes, G. R. Blumenthal an
inclusion of the gravitational
the centre of the halo can res
curve to the inner regions of t
largest objects in the simulati
similar to that of M31 and th
down to that of M33. Prior
massive binary had flat rotatio
and 260 km s^{-1}; at the final tim
coalesced. Their merged halo
asymptotic velocity of 350 km
energy of the remnant was in
pair. The slow rise within 60 k
top two rotation curves in Fi
the largest spirals.

During the initial collapse

Initial conditions

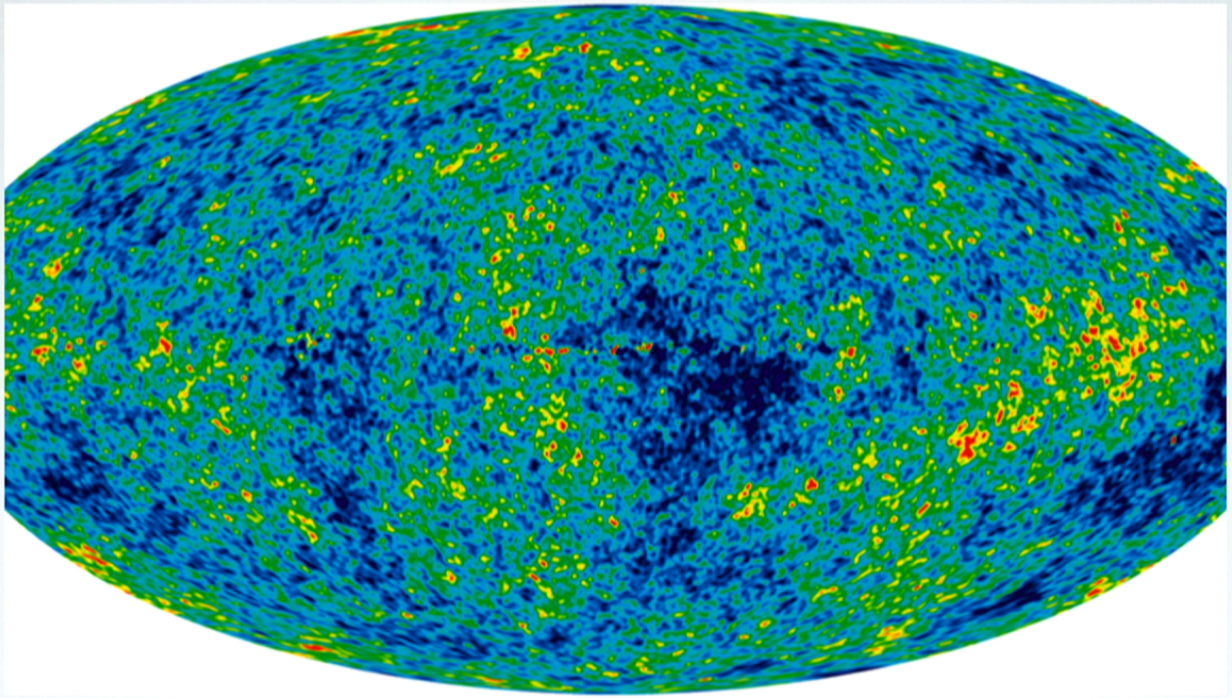

WMAP SCIENCE TEAM

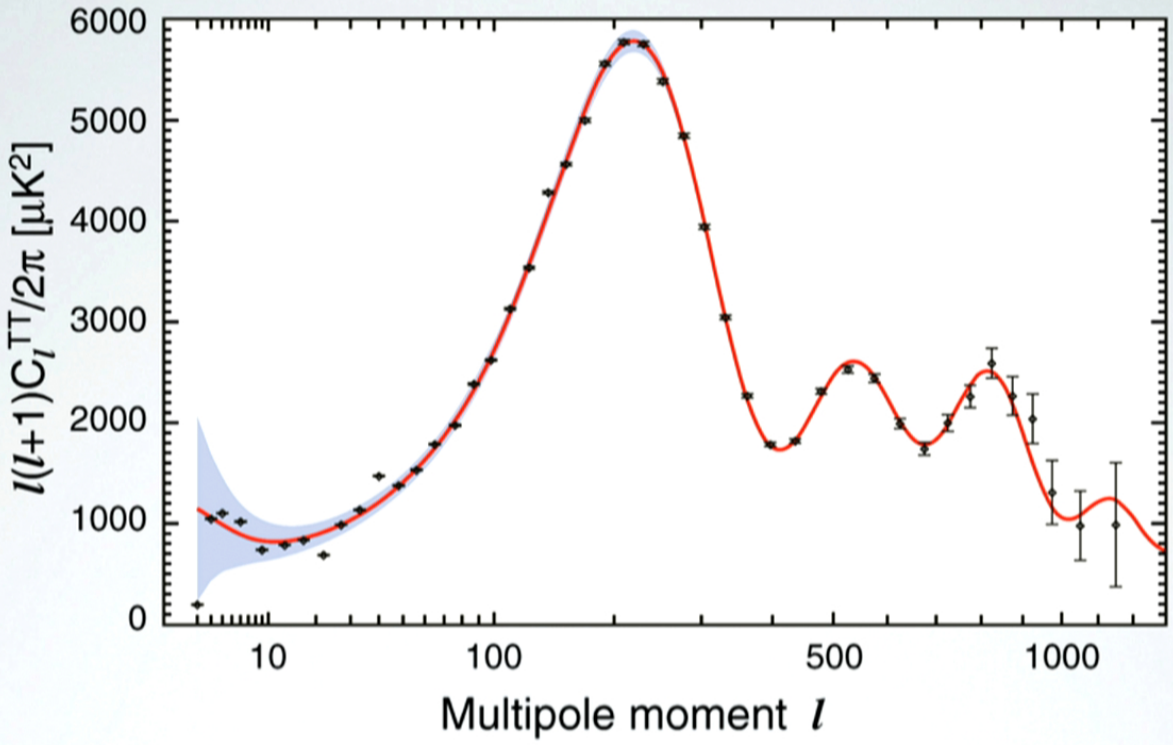

POWER SPECTRUM

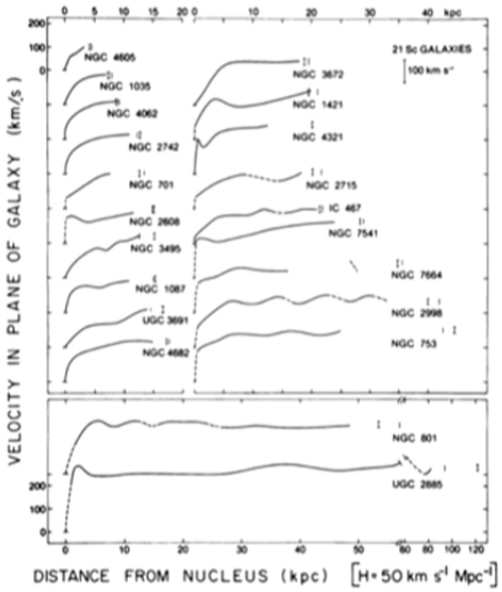

FIG. 5.—Mean velocities in the plane of the galaxy, as a function of linear distance from the nucleus for 21 Sc galaxies, arranged according to increasing linear radius. Curve drawn is rotation curve formed from mean of velocities on both sides of the major axis. Vertical bar marks the location of R_{25}, the isophote of 25 mag arcsec^{-2}; those with upper and lower extensions mark $R^{c,i}$, i.e., R_{25} corrected for inclination and galactic extinction. Dashed line from the nucleus indicates regions in which velocities are not available, due to small scale. Dashed lines at larger R indicates a velocity fall faster than Keplerian.

Dark Matter

Rubin et al. (1980) ApJ 238 471

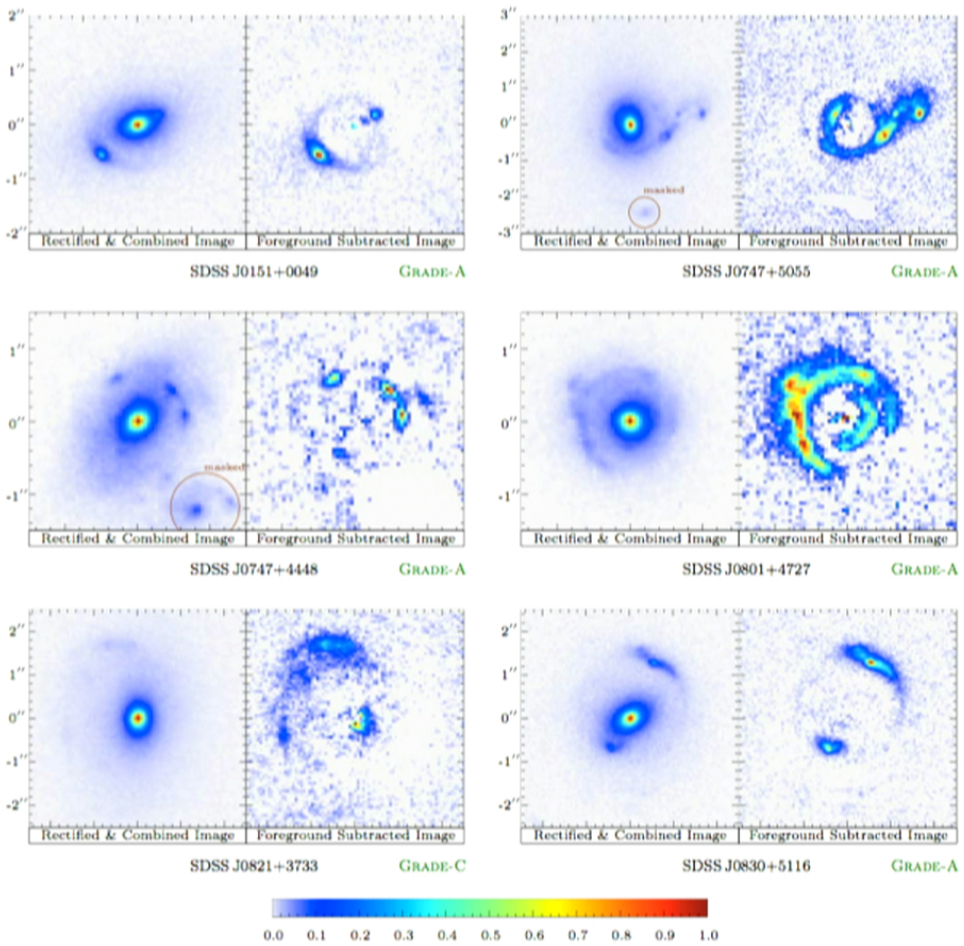

Figure 2. BELLS strong gravitational lens galaxies and foreground-subtracted images. The 36 grade-A, -B, and -C lenses discovered under *HST* cycle 18 program 12209. For each system, the left panel shows the *HST* ACS-WFC F814W rectified and combined images with north up and east to the left, and the right panel reveals the lensed features which remain after the foreground galaxy has been subtracted by the B-spline method described in Section 3. Probable non-lensed extraneous features that were masked are circled. System properties from the BOSS data are listed in Table 2, and those from the *HST*-ACS data are listed in Table 3. Comments justifying our lens grade are provided in Table 4.

Brute force and ignorance

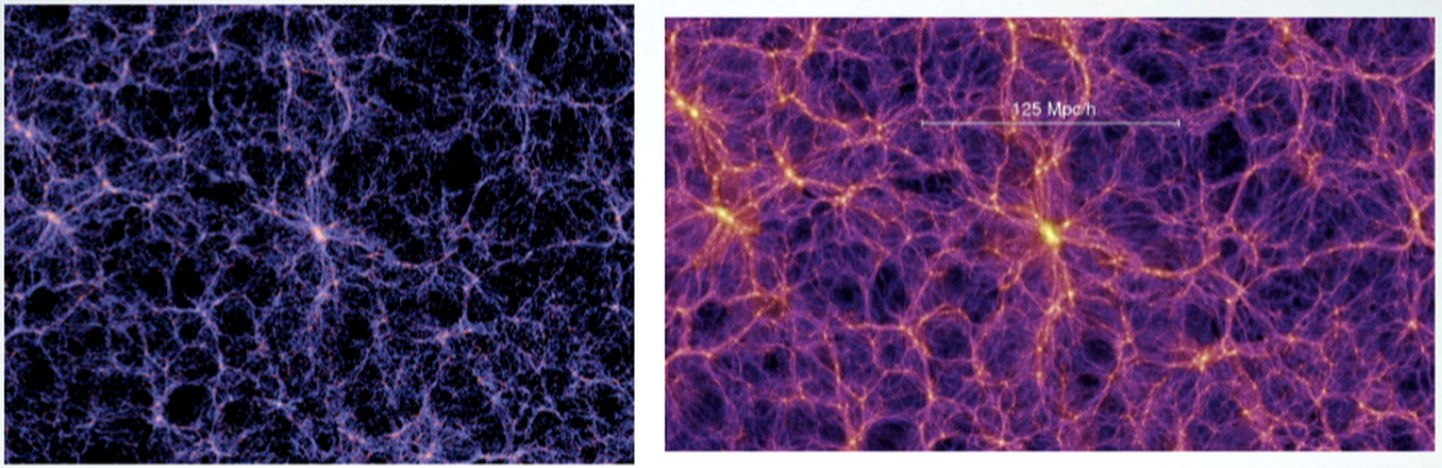

MILLENNIUM SIMULATION
GALAXIES ON THE LEFT DARK MATTER
ON THE RIGHT


Stars are easy to see
But they from only in halos, and they account for < 25% of the cosmic abundance in their host halos

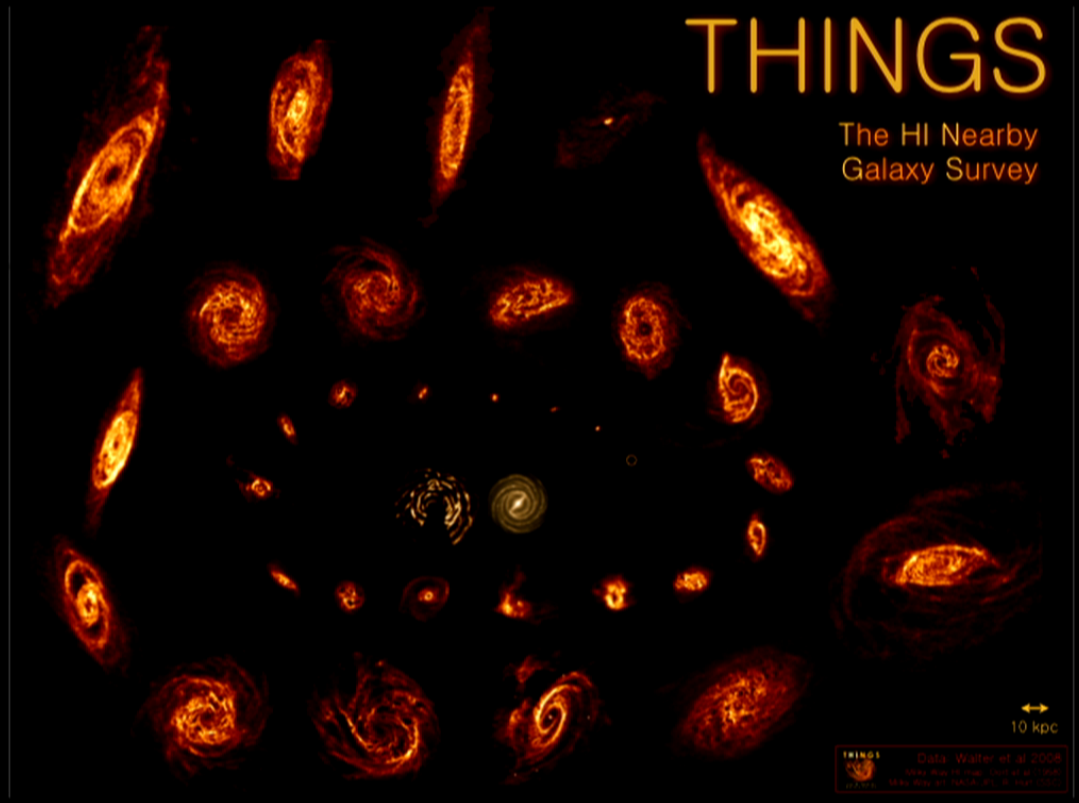

Neutral hydrogen

Is also easy to see, but accounts for < 10% of baryons

Dai et al. (2010)
ApJ, 719, 119

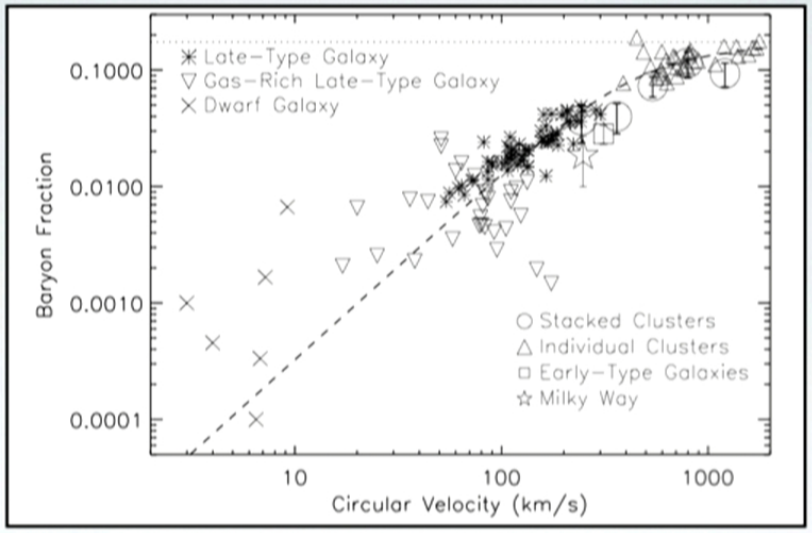

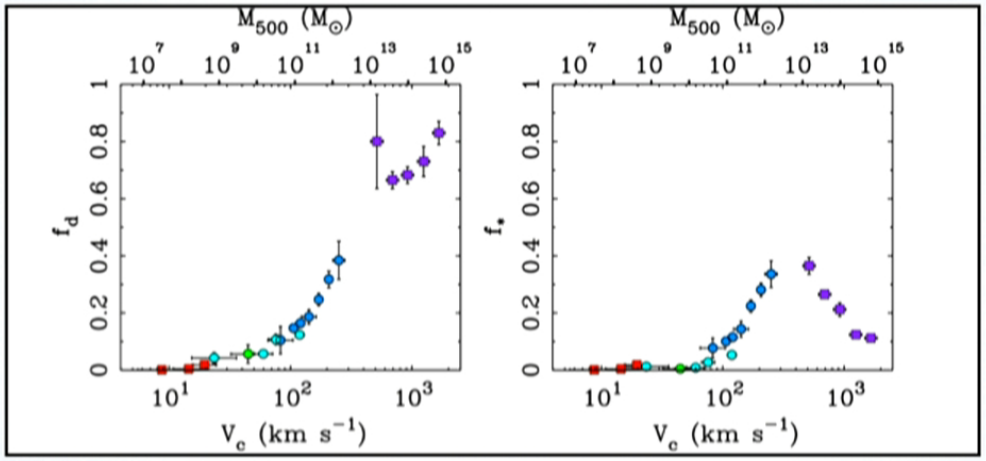

MCGAUGH ET AL. (2010) APJL, 708, 1

Where are the baryons?

Note: this is a low z problem only

STELLAR FEEDBACK

Supernovae, O star Winds, Radiative Heating,
Radiation Pressure

BLOWING UP GMCS IN COLOR 3D

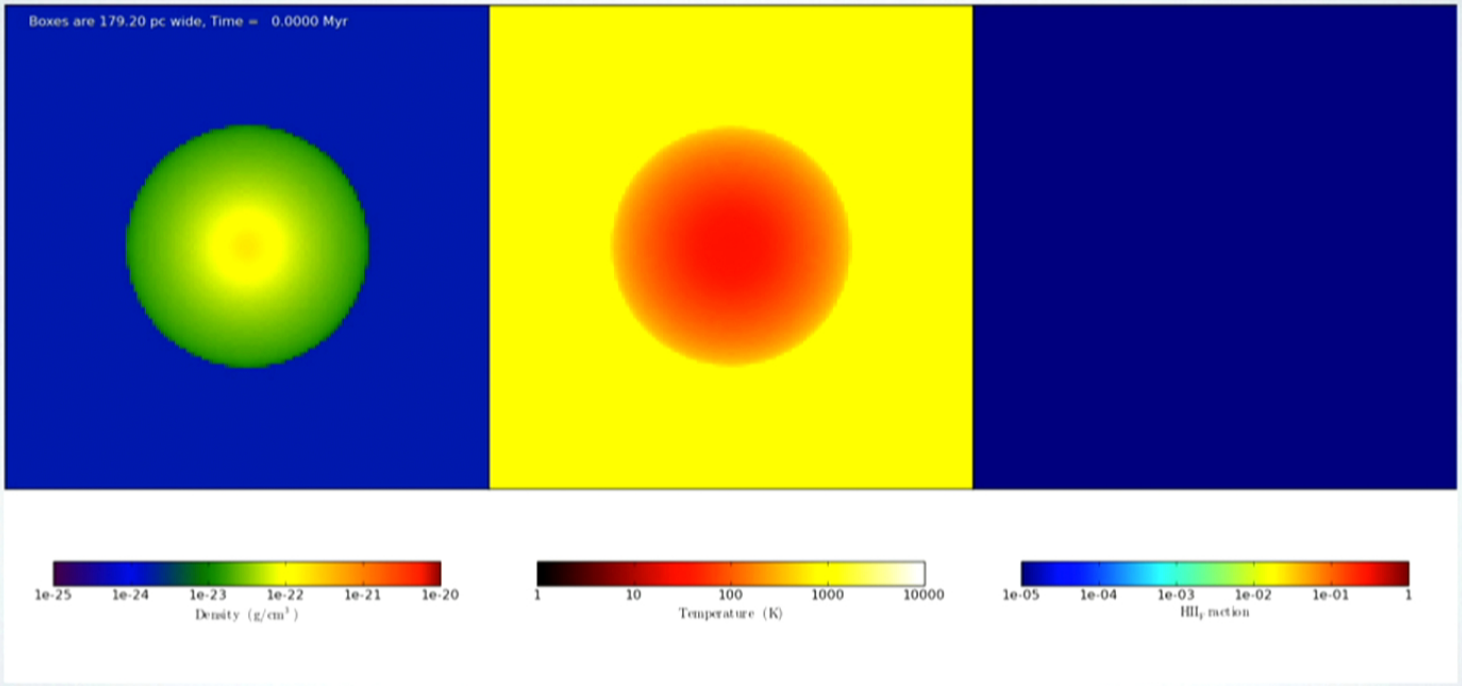

Harper-Clark; ENZO2 raytracing

BLOWING UP GMCS IN COLOR 3D

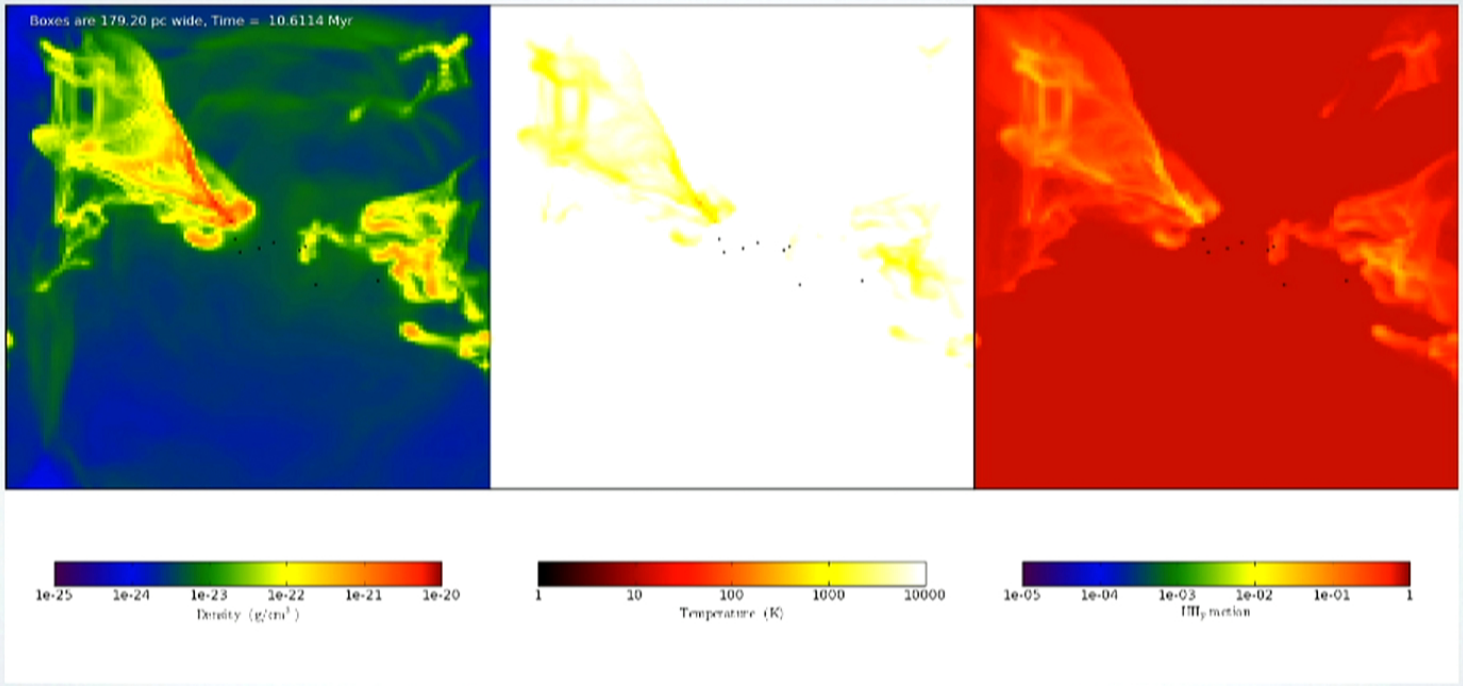

Harper-Clark; ENZO2 raytracing

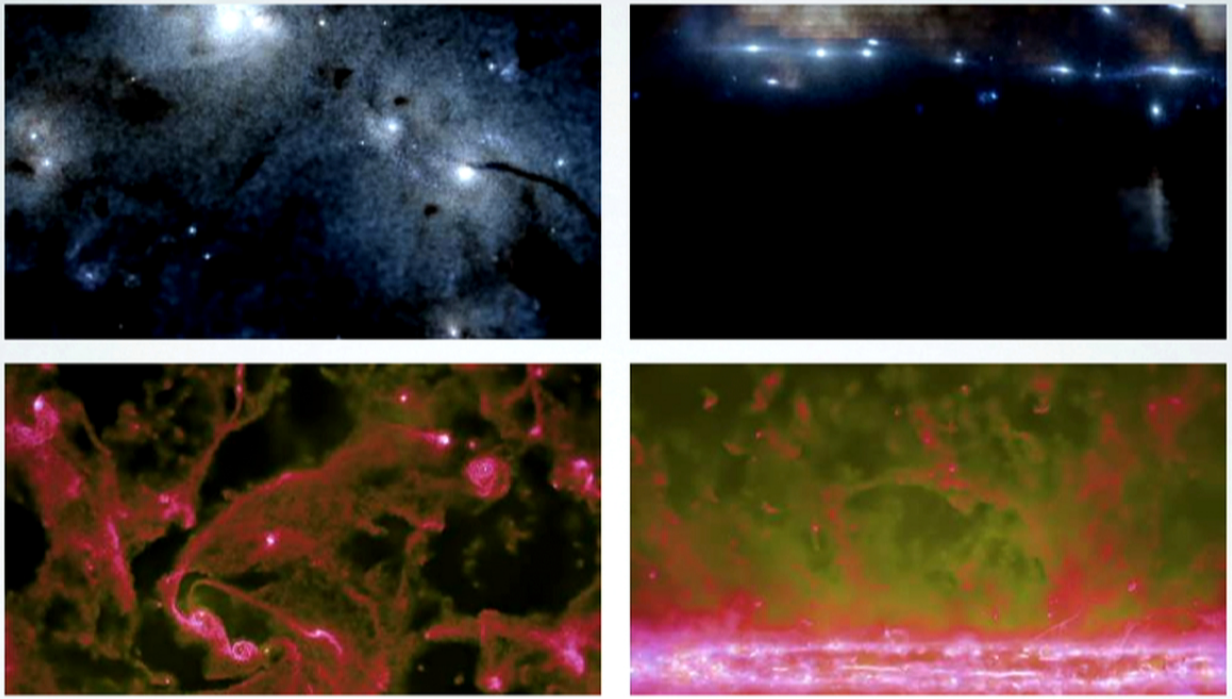

GALACTIC SCALE SIMULATIONS

FEEDBACK SLOWS STAR FORMATION AND DRIVES WINDS
HOPKINS, QUATAERT

Gadget (sph) & MFM (~moving grid)

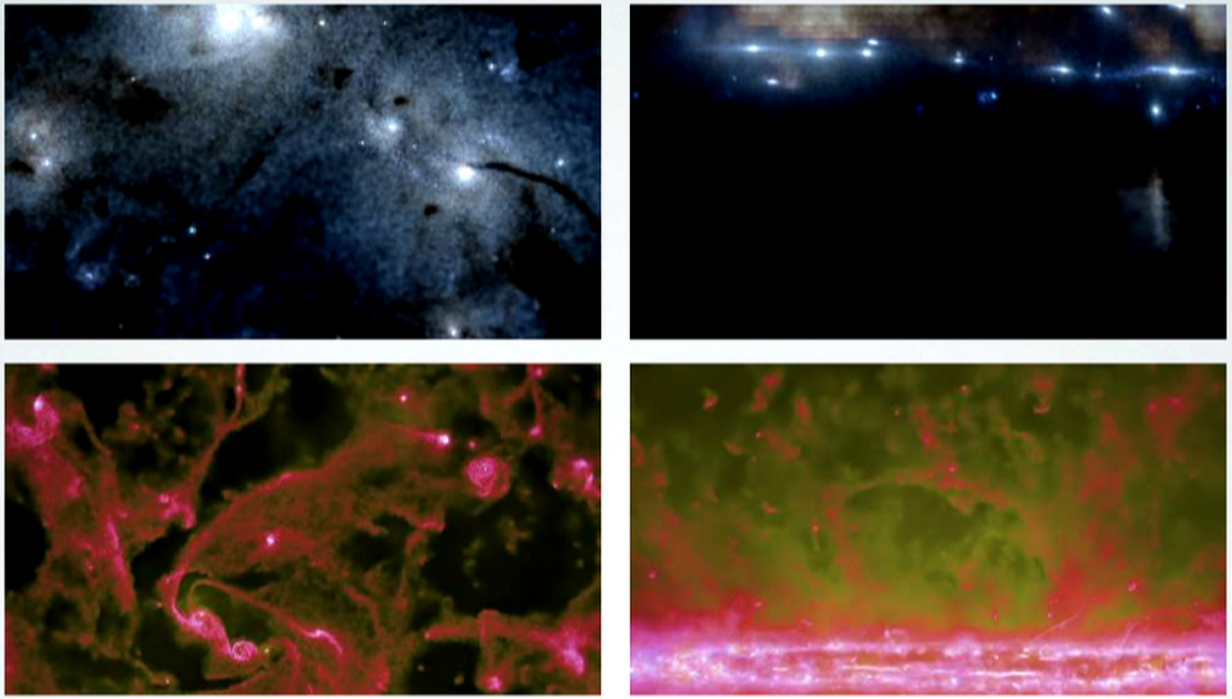

GALACTIC SCALE SIMULATIONS

FEEDBACK SLOWS STAR FORMATION AND DRIVES WINDS
HOPKINS, QUATAERT

Gadget (sph) & MFM (~moving grid)

Cosmological Simulations

FIRE: Feedback in Realistic Environments

Proto-MW: Gas Temperature:

No Feedback

Following Full Feedback

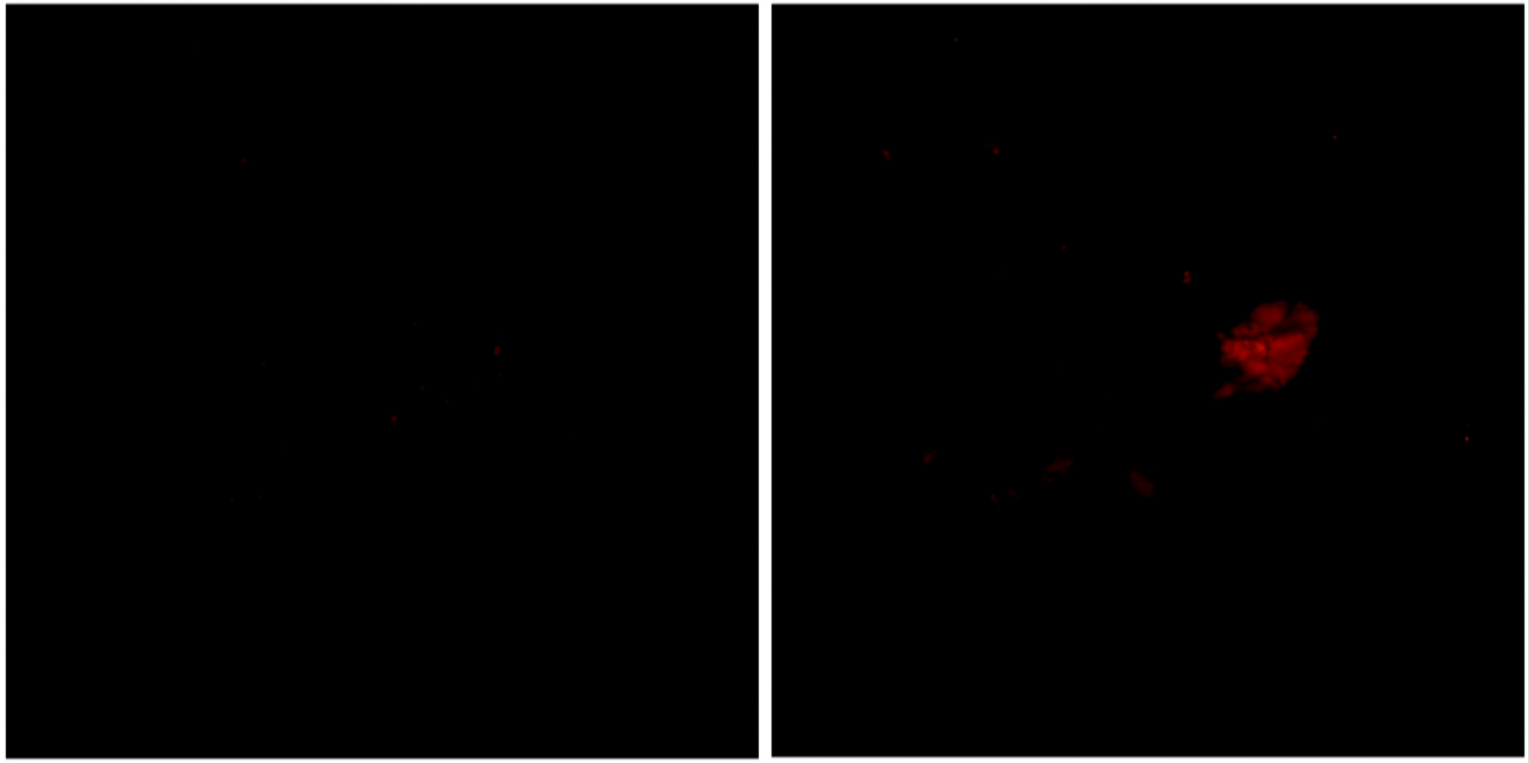

Hopkins et al. (2014) MNRAS 445 581

Cosmological Simulations

FIRE: Feedback in Realistic Environments

Proto-MW: Gas Temperature:

No Feedback

Following Full Feedback

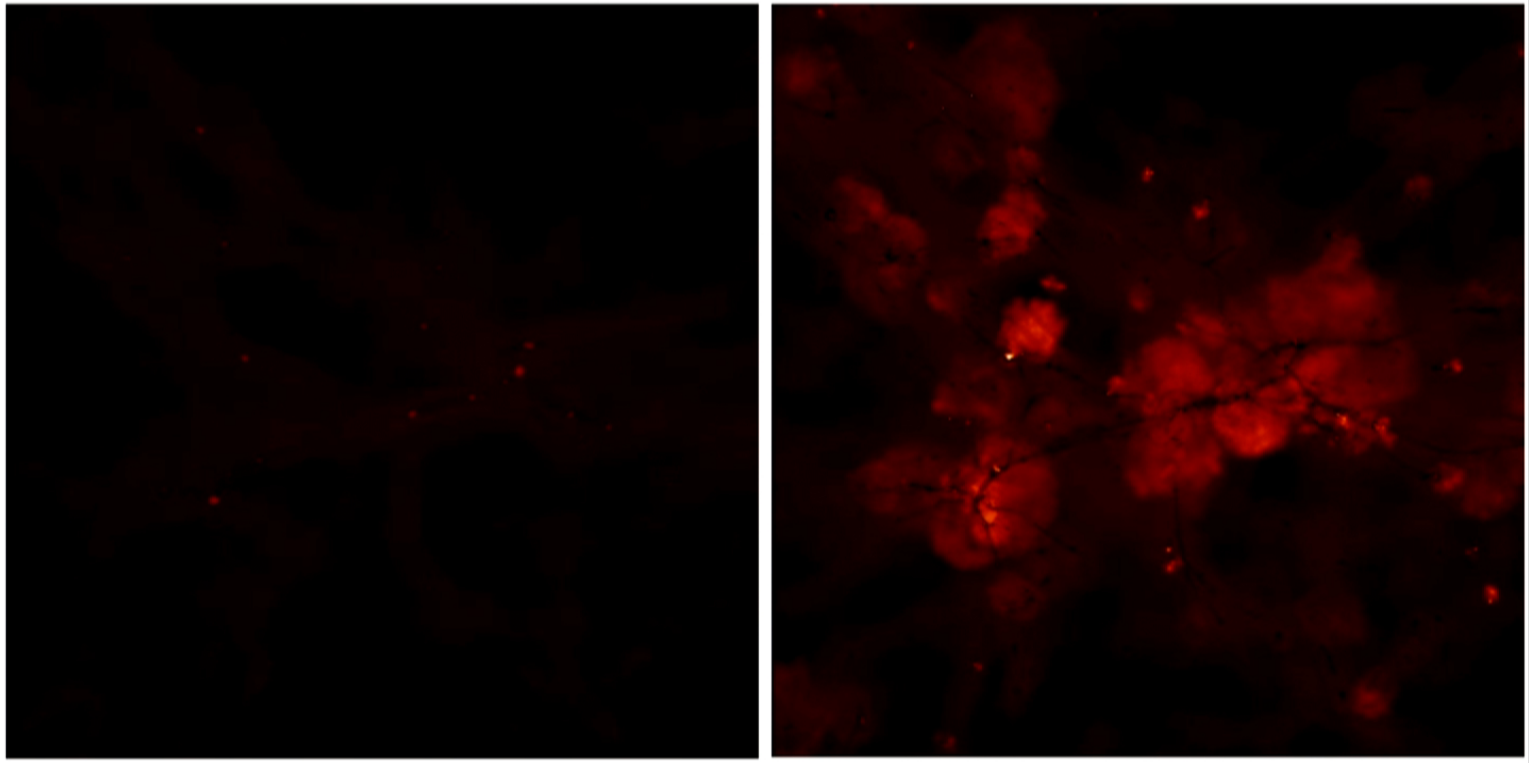

Hopkins et al. (2014) MNRAS 445 581

Cosmological Simulations

FIRE: Feedback in Realistic Environments

Proto-MW: Gas Temperature:

No Feedback

Following Full Feedback

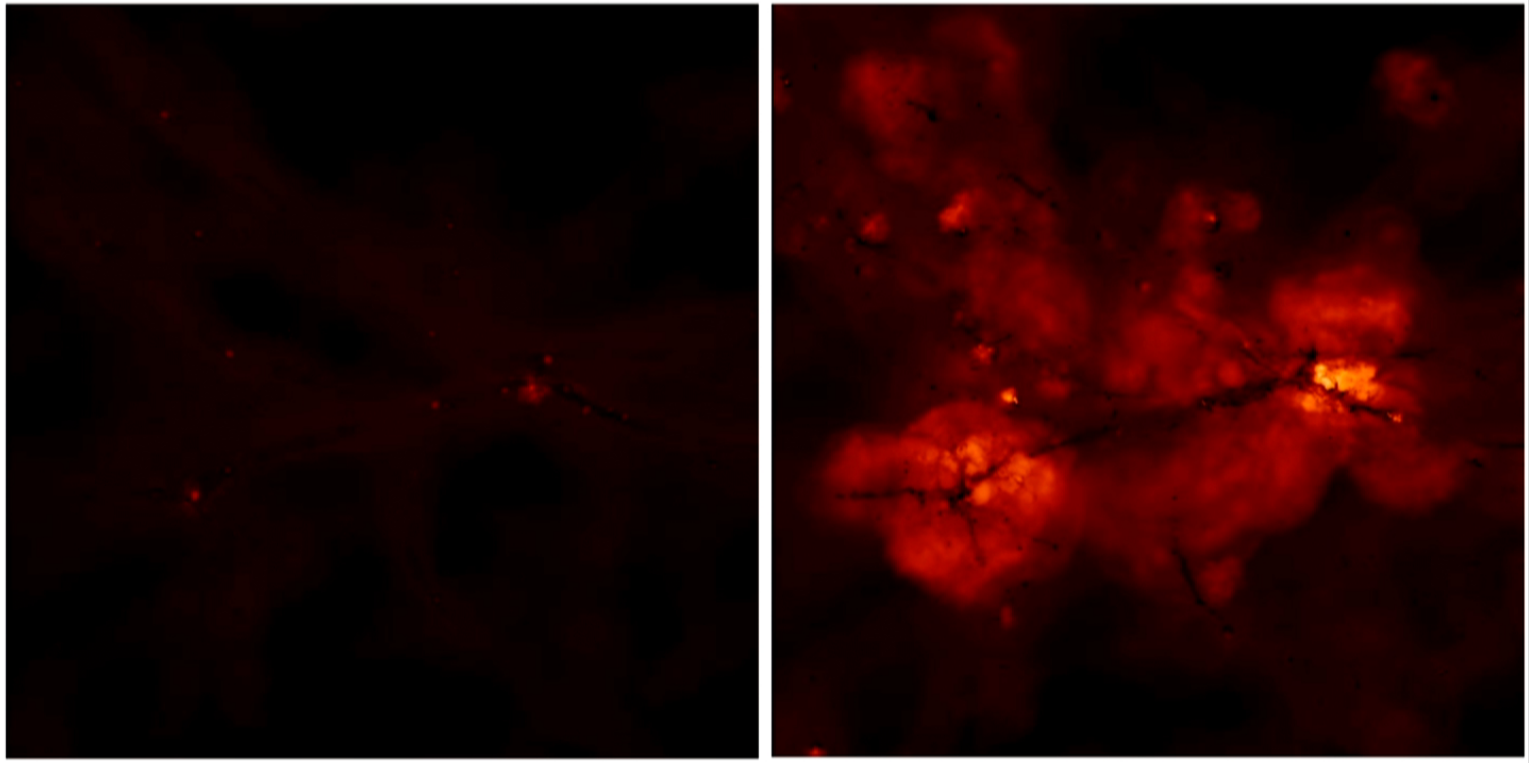

Hopkins et al. (2014) MNRAS 445 581

Cosmological Simulations

FIRE: Feedback in Realistic Environments

Proto-MW: Gas Temperature:

No Feedback

Following Full Feedback

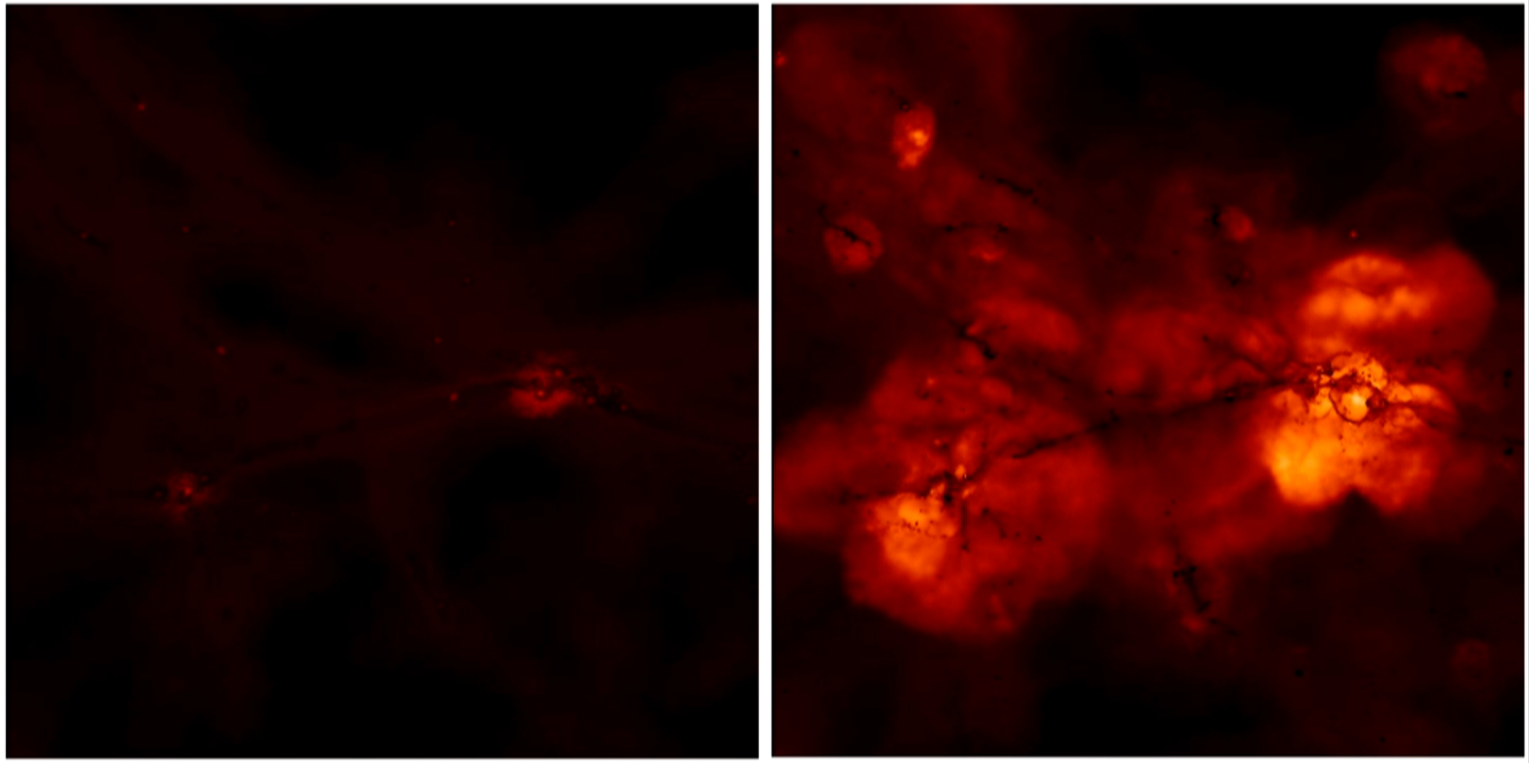

Hopkins et al. (2014) MNRAS 445 581

Cosmological Simulations

FIRE: Feedback in Realistic Environments

Proto-MW: Gas Temperature:

No Feedback

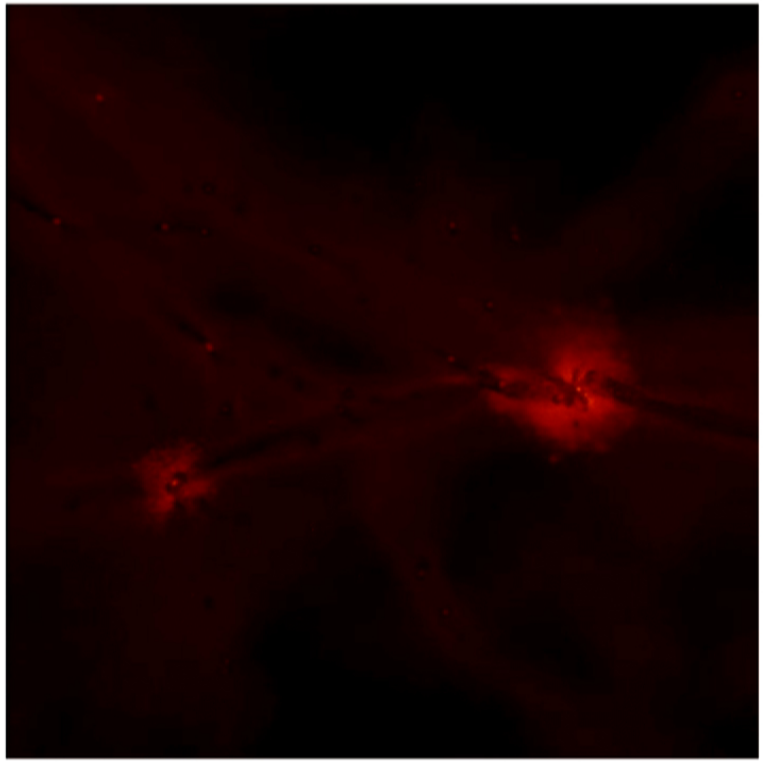

Following Full Feedback

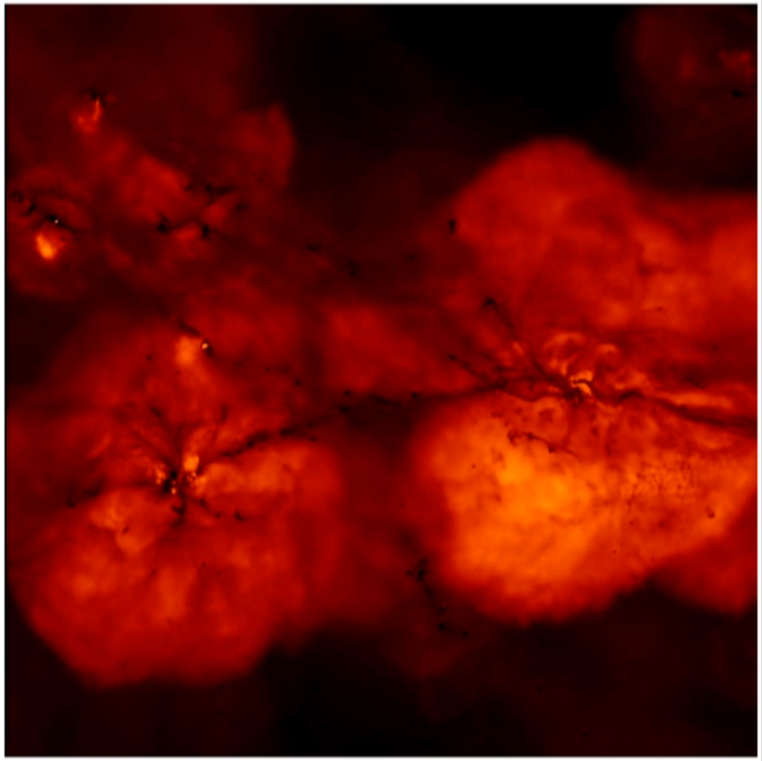

Hopkins et al. (2014) MNRAS 445 581

Cosmological Simulations

FIRE: Feedback in Realistic Environments

Proto-MW: Gas Temperature:

No Feedback

Following Full Feedback

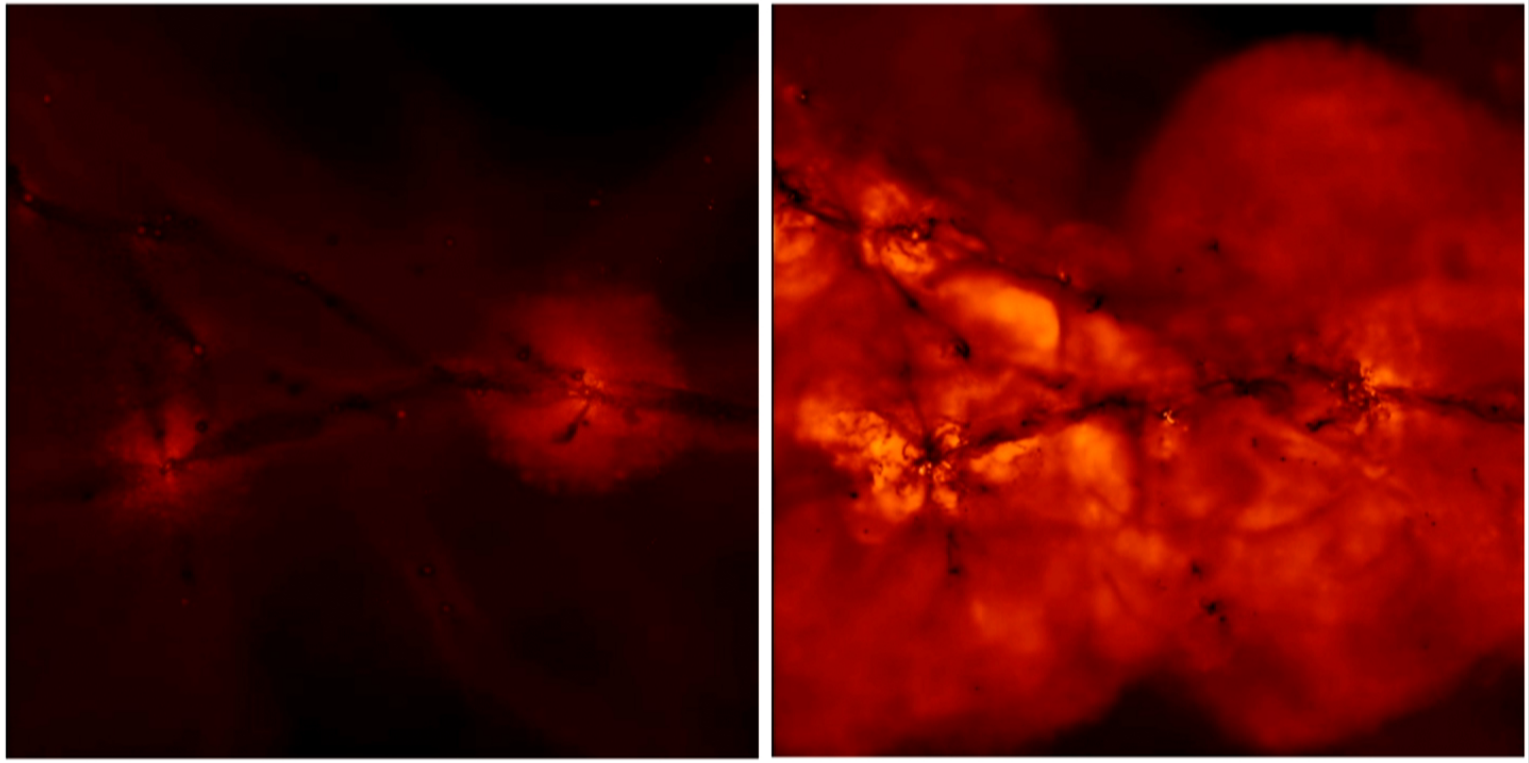

Hopkins et al. (2014) MNRAS 445 581

Cosmological Simulations

FIRE: Feedback in Realistic Environments

Proto-MW: Gas Temperature:

No Feedback

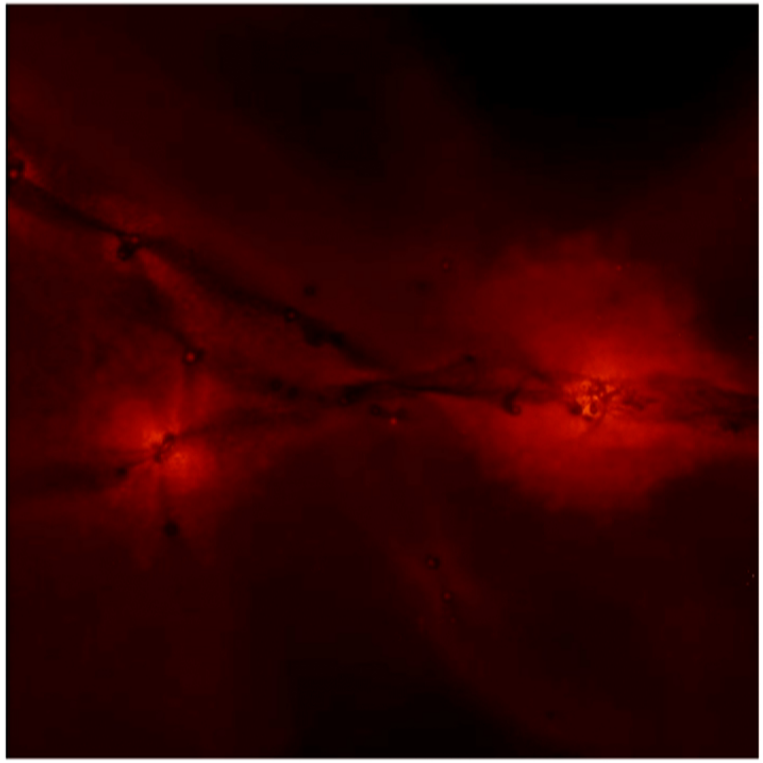

Following Full Feedback

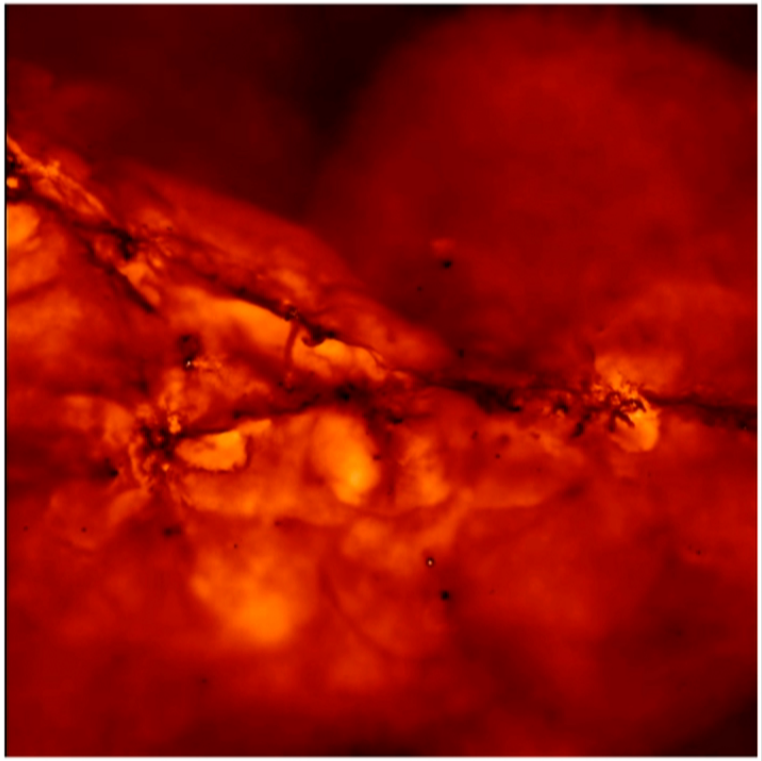

Hopkins et al. (2014) MNRAS 445 581

Cosmological Simulations

FIRE: Feedback in Realistic Environments

Proto-MW: Gas Temperature:

No Feedback

Following Full Feedback

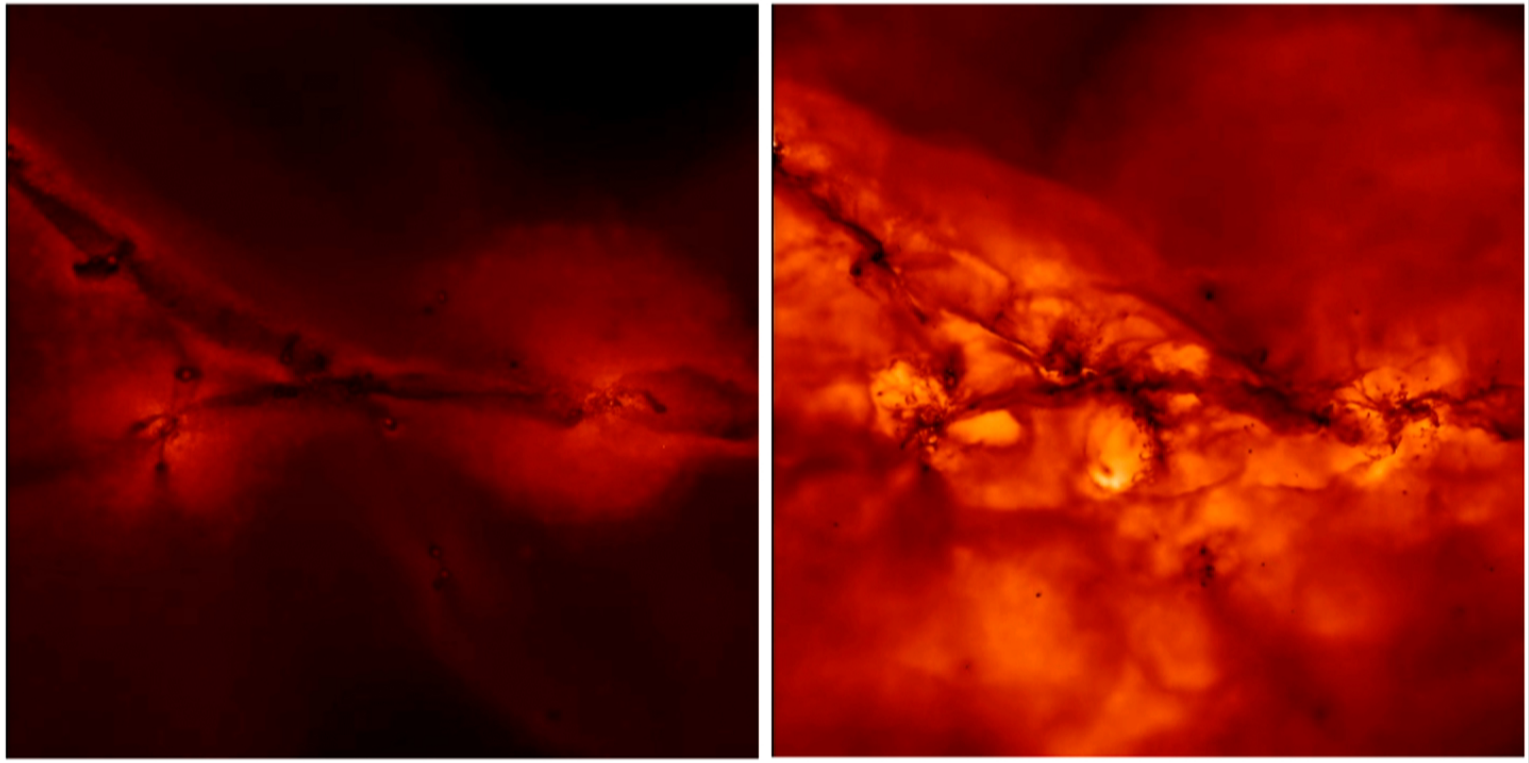

Hopkins et al. (2014) MNRAS 445 581

Cosmological Simulations

FIRE: Feedback in Realistic Environments

Proto-MW: Gas Temperature:

No Feedback

Following Full Feedback

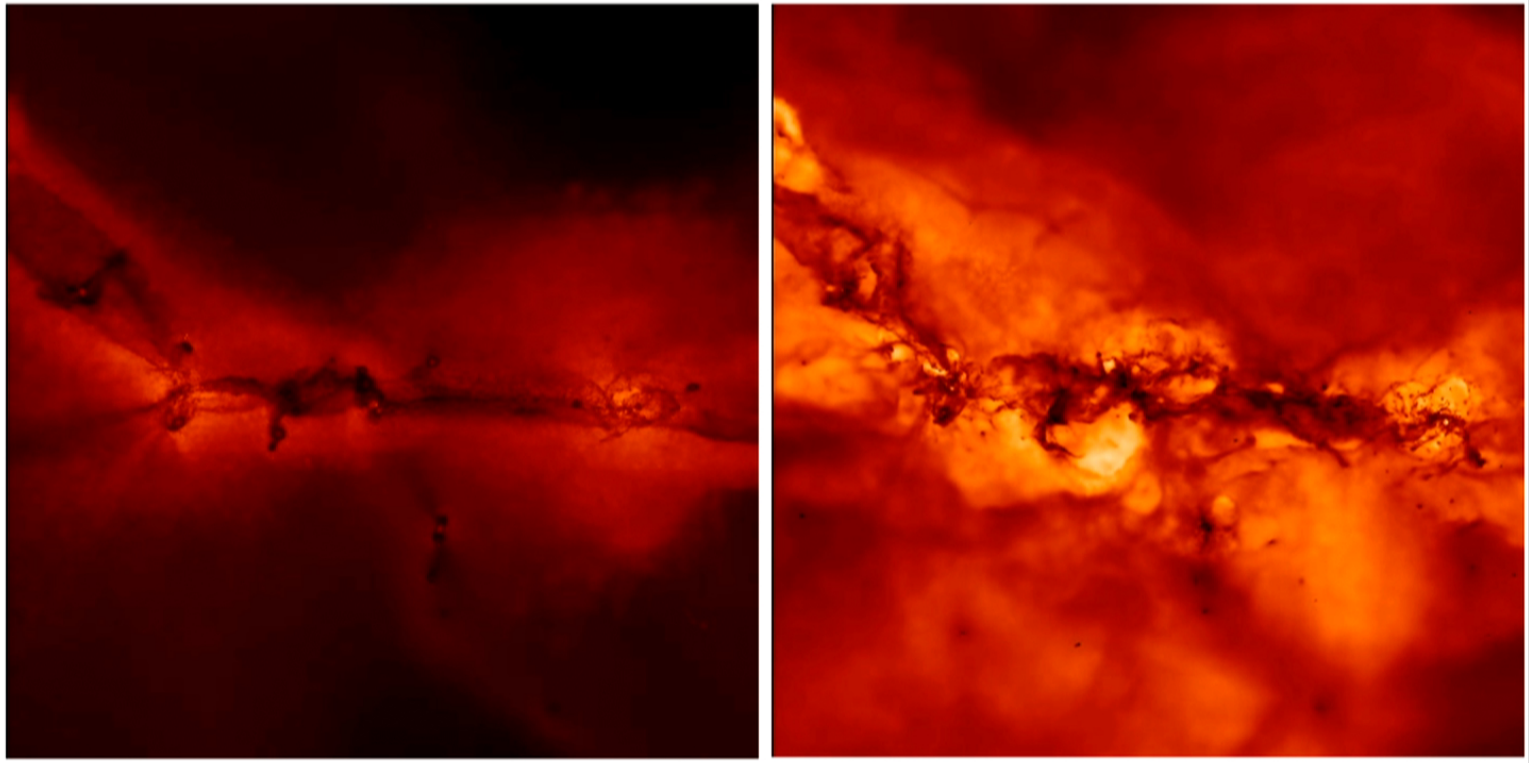

Hopkins et al. (2014) MNRAS 445 581

Cosmological Simulations

FIRE: Feedback in Realistic Environments

Proto-MW: Gas Temperature:

No Feedback

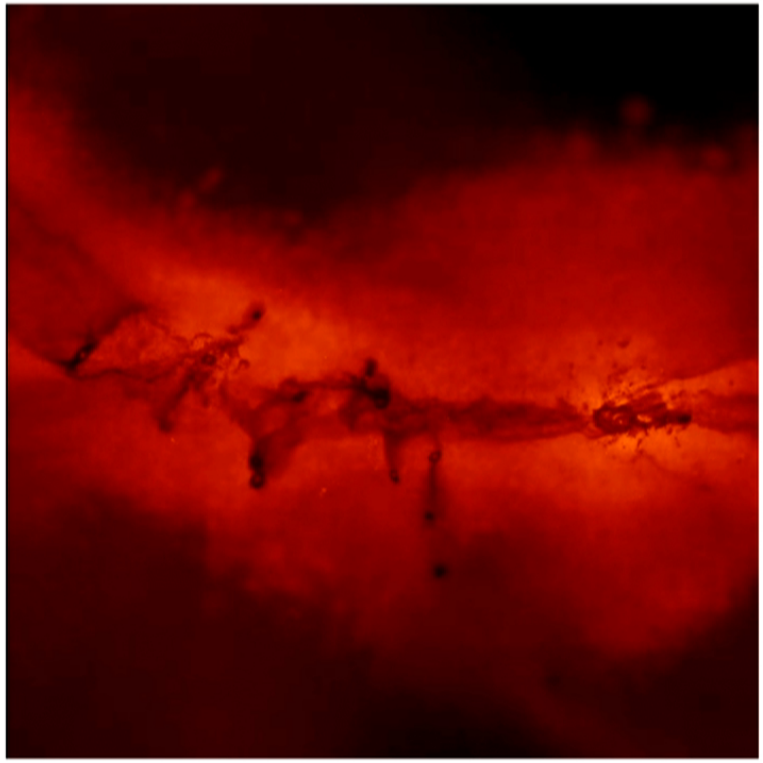

Following Full Feedback

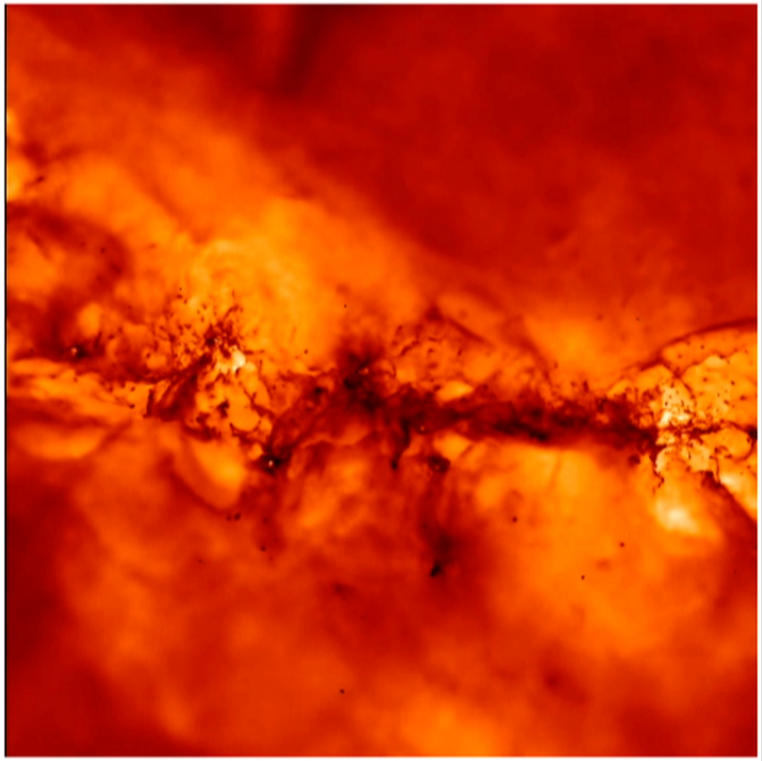

Hopkins et al. (2014) MNRAS 445 581

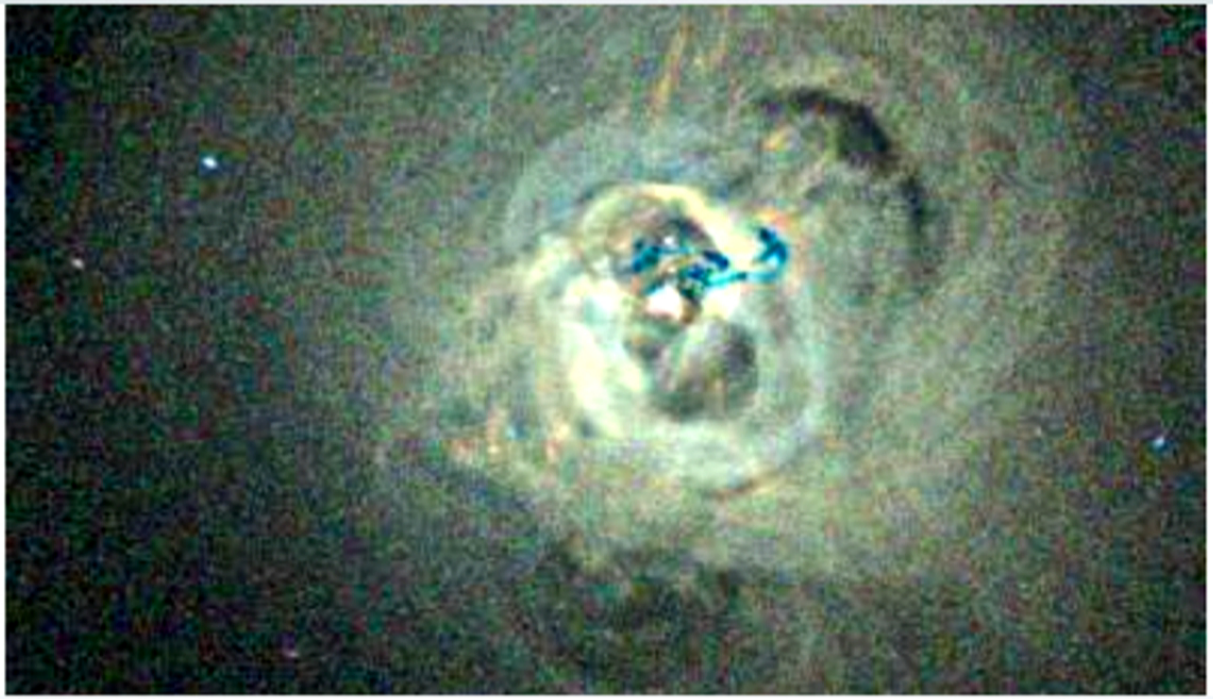

AGN FEEDBACK

Radio Jets, Broad Absorption Line Winds, Radiative Heating, Radiation Pressure

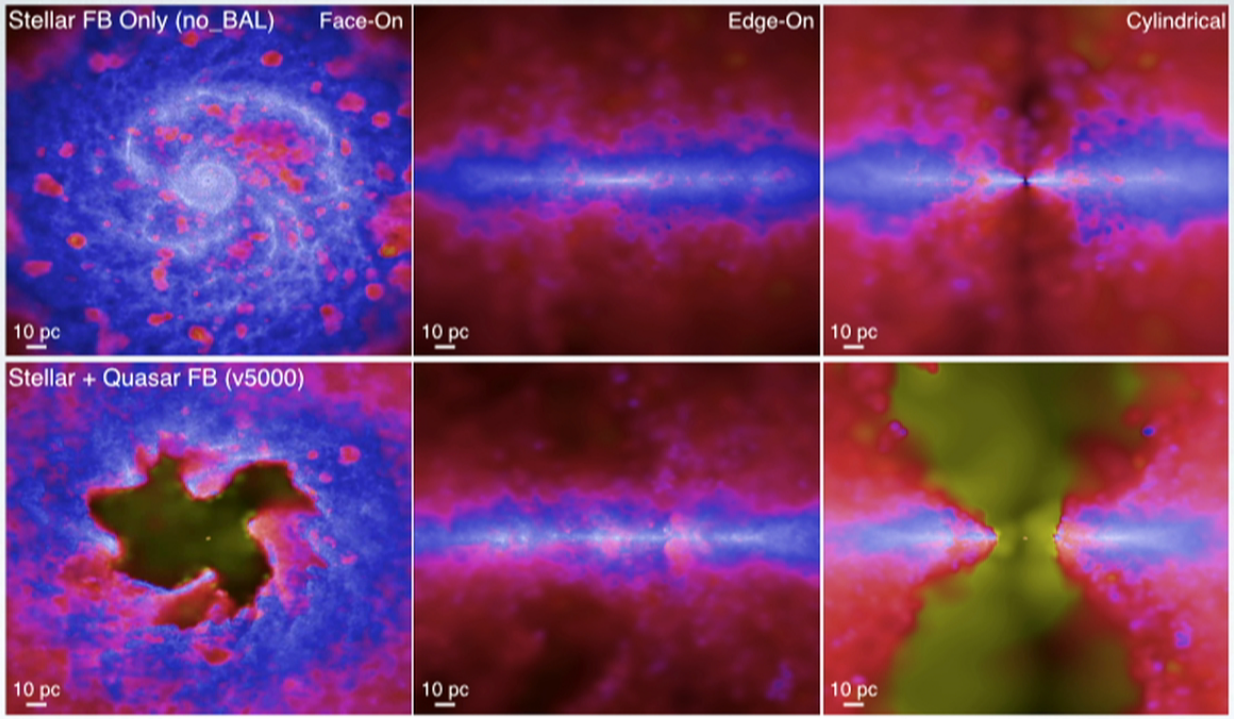

AGN FEEDBACK

BAL wind and radiative heating

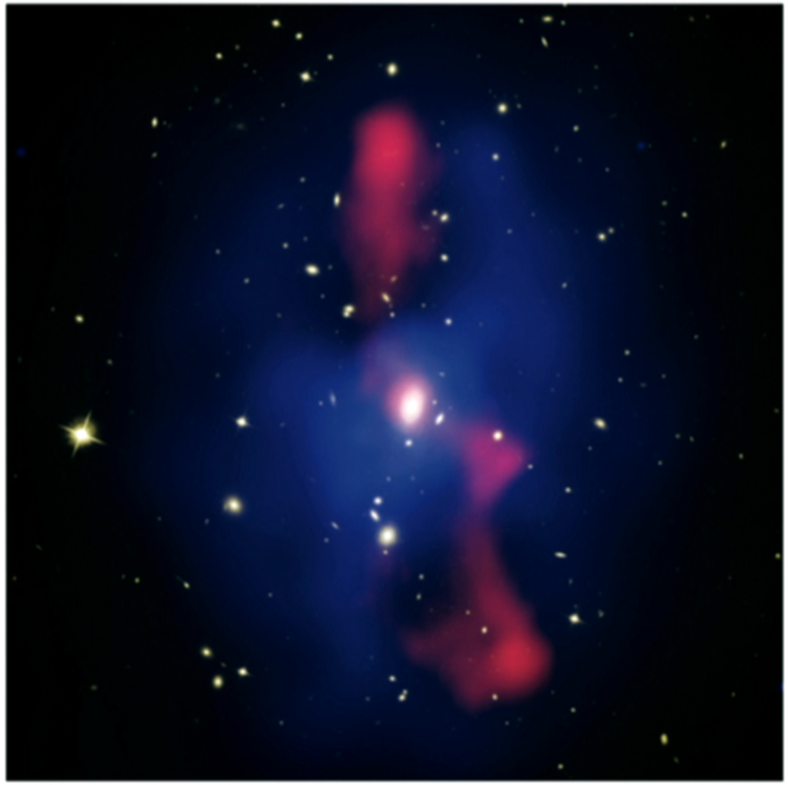

Figure 2

Hubble Space Telescope visual image of the MS0735.6+7421 cluster superposed with the *Chandra* X-ray image in blue and a radio image from the Very Large Array at a frequency of 330 MHz in red. The X-ray image shows an enormous pair of cavities, each roughly 200 kpc in diameter that are filled with radio emission. The radio jets have been inflating the cavities for 10^8 years with an average power of $<2 \times 10^{46}$ erg s^{-1}. The displaced gas mass is $<10^{12}$ $M_\odot$. The cavities and radio source are bounded by a weak shock front. The cavities are well outside the central galaxy and cooling region of the cluster. The supermassive black hole grew by at least $<3 \times 10^8$ $M_\odot$ during the outburst.

AGN FEEDBACK


So can we detect the baryons?
The ones in and around halos…

Detecting baryons in the form of diffuse gas

- Look for emission, e.g., x-rays
  - proportional to n^2
  - seen in massive cluster, and in stacks of smaller objects
- Sunyaev-Zeldovic (Compton scattering of CMB)
  - proportional to n_e

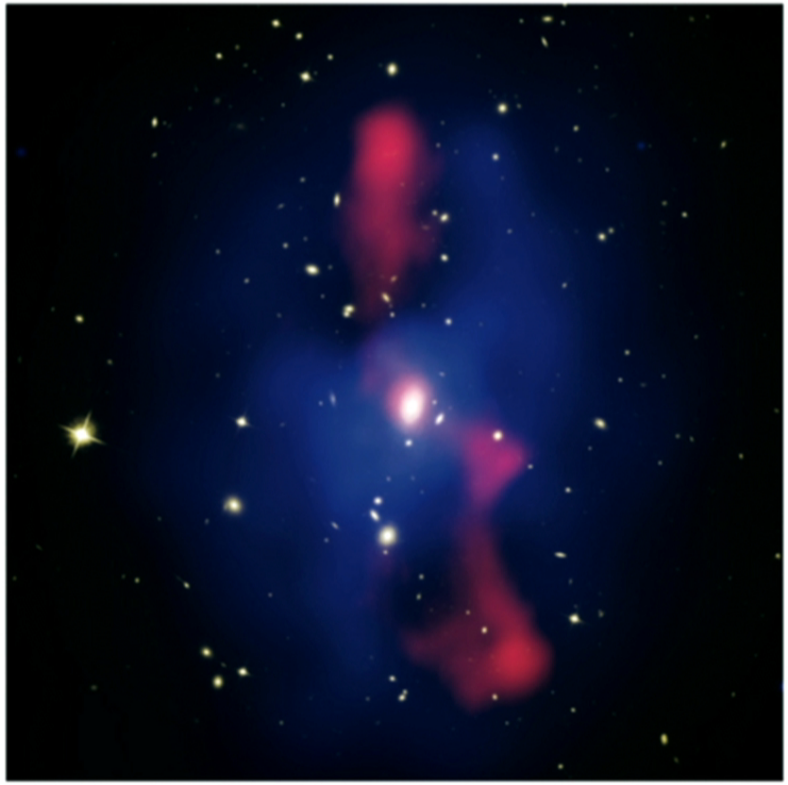

Figure 2

Hubble Space Telescope visual image of the MS0735.6+7421 cluster superposed with the *Chandra* X-ray image in blue and a radio image from the Very Large Array at a frequency of 330 MHz in red. The X-ray image shows an enormous pair of cavities, each roughly 200 kpc in diameter that are filled with radio emission. The radio jets have been inflating the cavities for 10^8 years with an average power of $<2 \times 10^{46}$ erg s^{-1}. The displaced gas mass is $<10^{12}$ $M_\odot$. The cavities and radio source are bounded by a weak shock front. The cavities are well outside the central galaxy and cooling region of the cluster. The supermassive black hole grew by at least $<3 \times 10^8$ $M_\odot$ during the outburst.

X-RAY EMISSION!

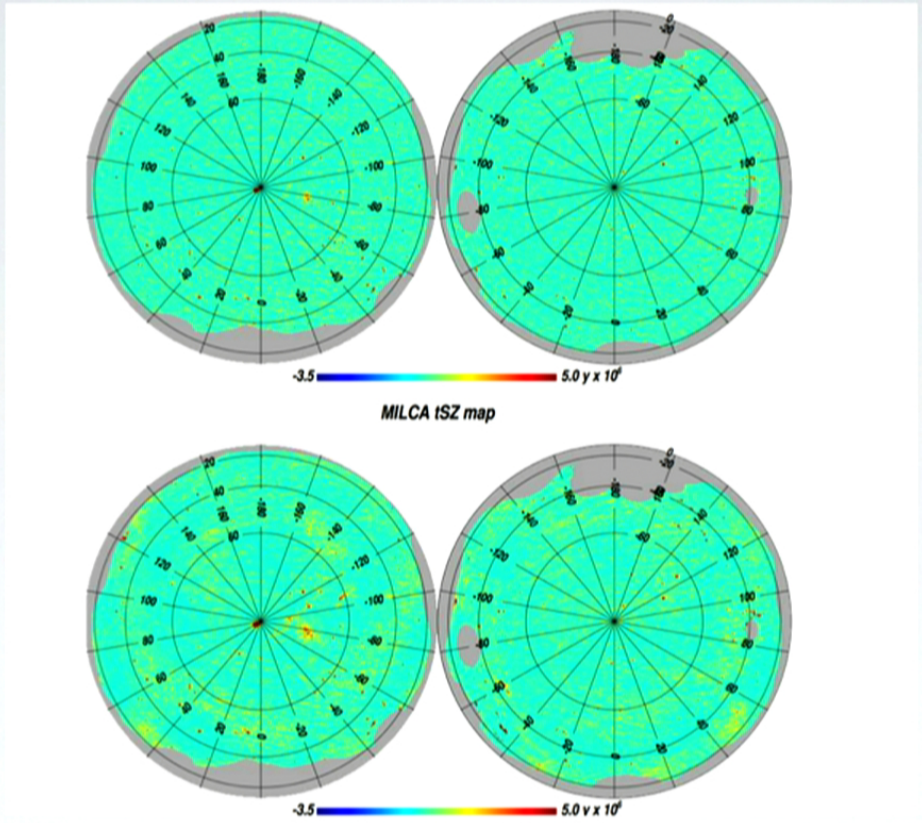

PLANCK 'Y' MAPS

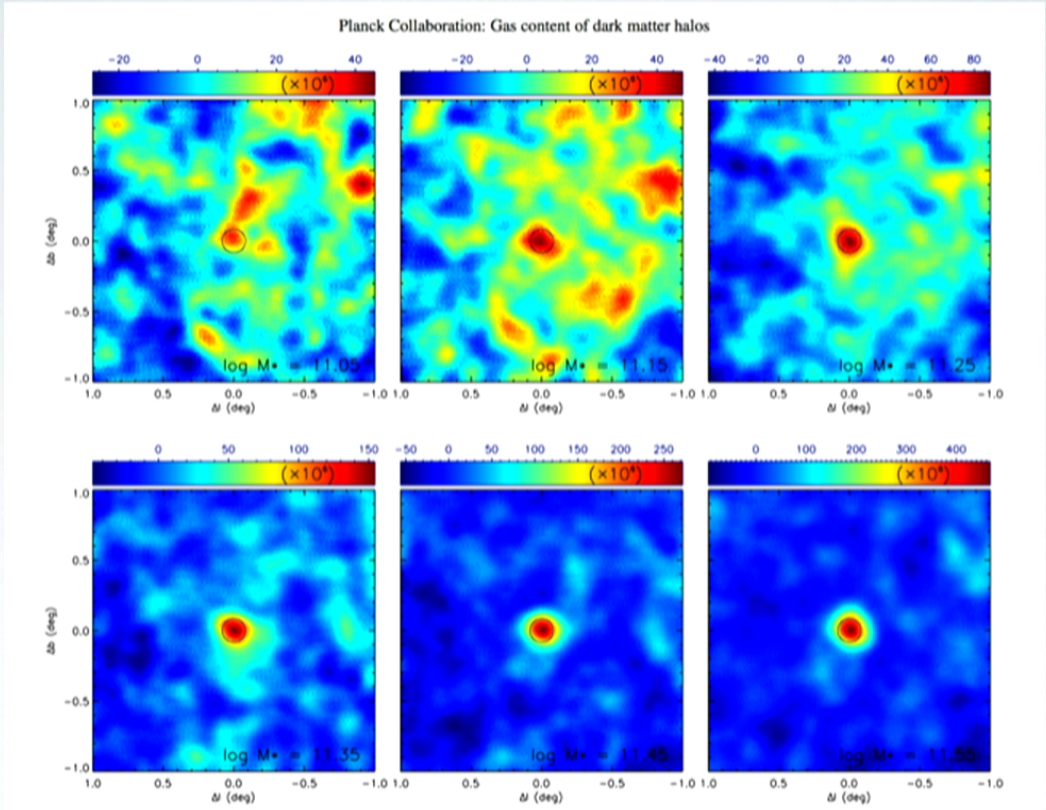

Fig. 5. Equal-weighted stacks of reconstructed SZ maps (i.e., Comptonization parameter maps) for objects in six mass bins centred, from *left to right* and *top to bottom*, at $\log_{10}(M_\star/M_\odot)$ = [11.05, 11.15, 11.25, 11.35, 11.45, 11.55]. In all cases, the bin size is taken to be 0.2, so the galaxies in two consecutive panels partially overlap. Maps are 2° on a side, with Galactic north at the top. The SZ signal traced by the central galaxies is clearly detected in all bins above $\log_{10}(M_\star/M_\odot) = 11.25$. In all panels, the circles indicate the FWHM of the data, which corresponds to 10′.

PLANCK XI

Do baryons (in the form of diffuse gas) trace the dark matter?

- Cross-correlate SZ maps with lensing maps

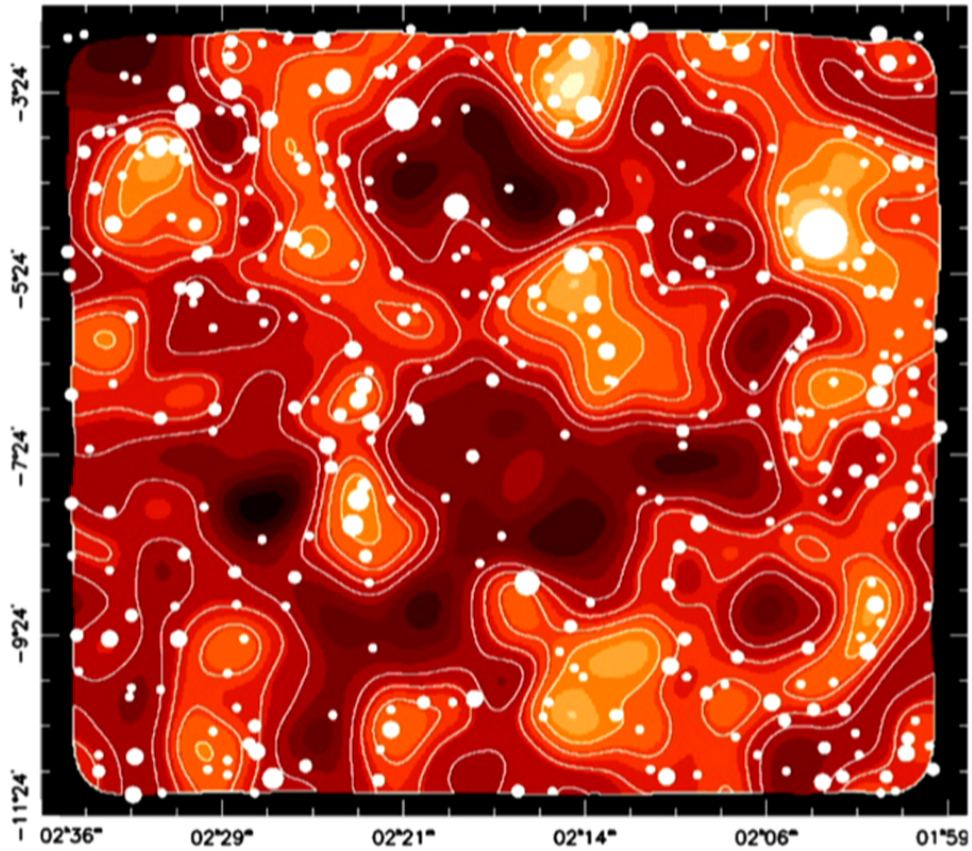

Figure 8. Mass maps for the W1 field. The continuous map with contours shows the mass reconstructed from gravitational lensing. The contours indicate the 1σ, 2σ, 3σ and 4σ on this map, where σ is the rms of the convergence. The open circles indicate the position of peaks in the predicted mass map, constructed from galaxies as described in Section 4.3. The circle size is proportional to the peak height. The field of view is approximately $9 \times 8\,\mathrm{deg}^2$.

Van Waerbeke et al (2013) MNRAS 433 3373

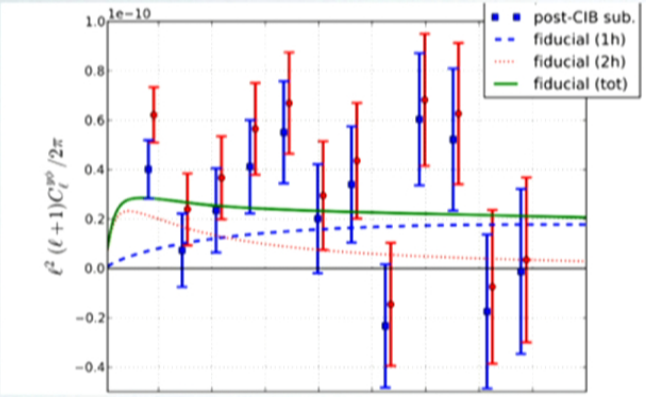

Hill & Spergel

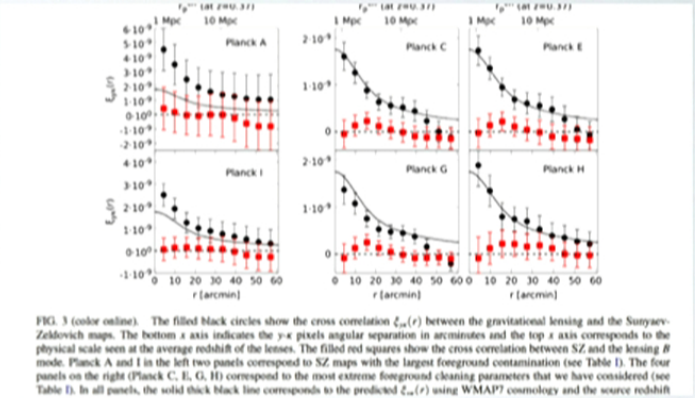

FIG. 3 (color online). The filled black circles show the cross correlation $\xi_{\kappa y}(r)$ between the gravitational lensing and the Sunyaev-Zeldovich maps. The bottom x axis indicates the y-κ pixels angular separation in arcminutes and the top x axis corresponds to the physical scale seen at the average redshift of the lenses. The filled red squares show the cross correlation between SZ and the lensing B mode. Planck A and I in the left two panels correspond to SZ maps with the largest foreground contamination (see Table I). The four panels on the right (Planck C, E, G, H) correspond to the most extreme foreground cleaning parameters that we have considered (see Table I). In all panels, the solid thick black line corresponds to the predicted $\xi_{\kappa y}(r)$ using WMAP7 cosmology and the source redshift

van Waerbeke, Hinshaw, & Murray

(LENSING) MASS-SZ CROSS CORRELATION

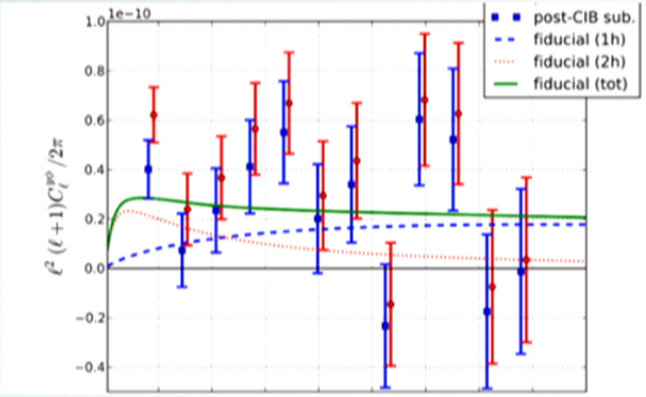

Hill & Spergel

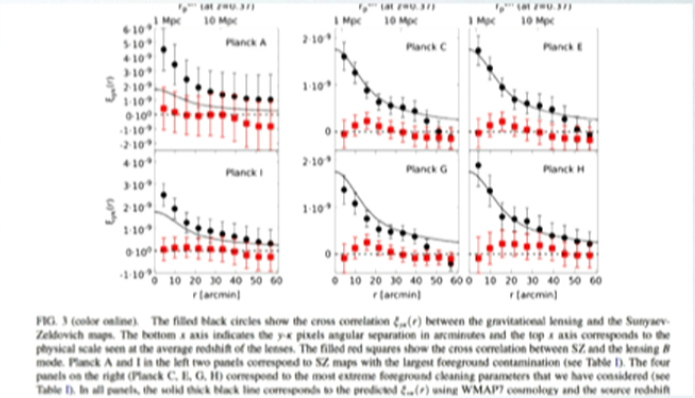

FIG. 3 (color online). The filled black circles show the cross correlation $\xi_{\kappa y}(r)$ between the gravitational lensing and the Sunyaev-Zeldovich maps. The bottom x axis indicates the y-κ pixels angular separation in arcminutes and the top x axis corresponds to the physical scale seen at the average redshift of the lenses. The filled red squares show the cross correlation between SZ and the lensing B mode. Planck A and I in the left two panels correspond to SZ maps with the largest foreground contamination (see Table I). The four panels on the right (Planck C, E, G, H) correspond to the most extreme foreground cleaning parameters that we have considered (see Table I). In all panels, the solid thick black line corresponds to the predicted $\xi_{\kappa y}(r)$ using WMAP7 cosmology and the source redshift

van Waerbeke, Hinshaw, & Murray

(LENSING) MASS-SZ CROSS CORRELATION

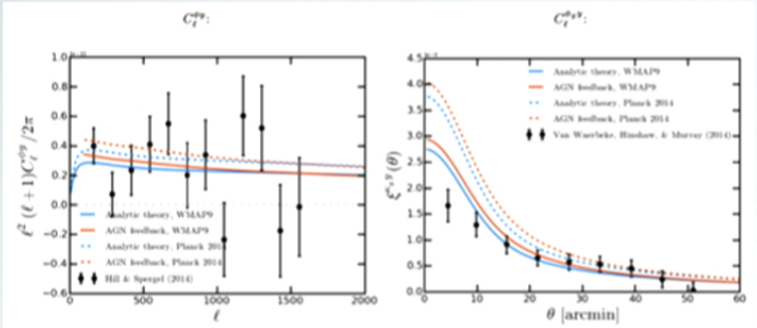

FIG. 7.— Comparison of the cross-spectra from the *AGN feedback* simulations and analytic halo model calculations to the observational results from Hill & Spergel (2014) and Van Waerbeke et al. (2014). In the right panel, we convert the theoretical results to the real-space cross-correlation function $\xi^{\kappa_{\rm CMB}y_{\rm tSZ}}(\theta)$ from Van Waerbeke et al. (2014). Both measurements prefer a lower amplitude than that predicted by the *Planck* cosmological parameters. Note that the multipole-space $C_\ell^{y_{\rm tSZ}y_{\rm tSZ}}$ data points in the left panel are nearly uncorrelated from bin to bin, while the real-space $\xi^{\kappa_{\rm CMB}y_{\rm tSZ}}$ data points in the right panel are strongly correlated.

Battaglia, Hill, & Murray

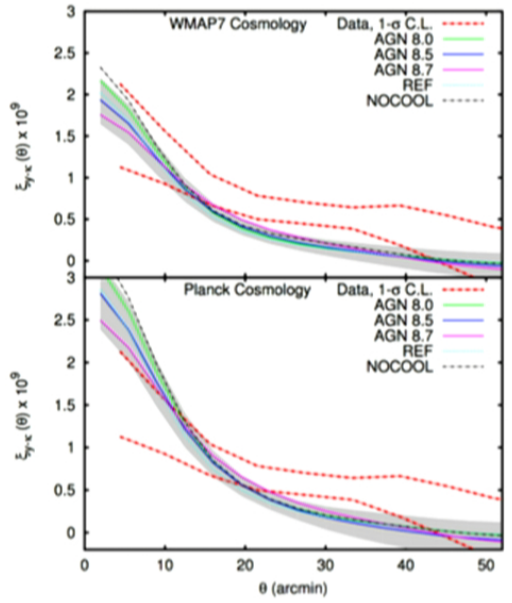

FIG. 1. Comparison of the cross-correlation function $\xi_{y\kappa}$ computed from hydrodynamical simulations to the signal detected in [7]. Per Table I, five different baryon feedback models are considered. The grey band represents the error on the mean

Hojjati et al.

(LENSING) MASS-SZ CROSS CORRELATION

A detection is nice. What can we do with it?
Future work

- Cross-correlation amplitude ~ $\sigma_8^{6.1}\,\Omega_m^{1.5}$ (Hill & Spergel)
  - constrain σ_8
- Learn about the cluster physics
- Locate the missing baryons—-maybe